Available online at www.sciencedirect.com
ScienceDirect
Trans. Nonferrous Met. Soc. China 26(2016) 1222−1231
Transactions of Nonferrous Metals Society of China
www.tnmsc.cn

Tensile fracture behavior of AA7075 alloy produced by thixocasting

Volkan KILICLI, Neset AKAR, Mehmet ERDOGAN, Kadir KOCATEPE

Department of Metallurgical and Materials Engineering, Faculty of Technology, Gazi University, 06500 Teknikokullar, Ankara, Turkey

Received 22 June 2015; accepted 20 November 2015

Abstract: Tensile fracture behaviors of thixocast, artificially aged thixocast (thixocast+T6) and as-extruded AA7075 alloys were investigated. The microstructural and fractographic observations were carried out using optical microscope (OM) and scanning electron microscope (SEM). Experimental studies showed that as-extruded and thixocast+T6 specimens exhibited considerably more excellent mechanical properties than as-thixocast AA7075 specimen. T6 artificial heat treatment with prolonged solution treatment significantly improved the tensile properties of the thixocast AA7075 alloy. The tensile properties of as-extruded and thixocast+T6 specimens were close to each other. In as-thixocast specimen having remarkable micro-cracks, fracture was intergranular brittle type. The ductile fracture surfaces were observed in as-extruded and thixocast+T6 specimens. In as-thixocast specimens, decohesion started between the eutectic−matrix interfaces and propagated through grains. Micro-void coalescence was the dominant form of fracture in thixocast+T6 heat treated specimens. The micro-voids nucleation was initiated at the interface between the matrix and multinary eutectic structure.

Key words: AA7075 alloy; semi-solid processing; thixocasting; tensile fracture behavior; tensile properties

1 Introduction

AA7075 aluminum alloys having essentially zinc, copper and magnesium, provide the highest strength of any commercial aluminum alloys. AA7075 aluminum alloy is heat treatable to obtain yield strength of 505 MPa and elongation of 11%, and commonly used for its mechanical properties in various fields like aircraft and automobile industry or aerospace engineering [1,2].

Most of the wrought high strength aluminum alloys are machined, extruded or rolled for mass production. These manufacturing methods are expensive and need complex tools or machines. Another disadvantage of this method is the massive waste materials during machining operation [3−8]. The wrought high strength aluminum alloys are not well suited for conventional casting due to tendency for hot cracking during solidification [9,10]. Thixocasting process is a semi-solid metal processing (SSP), which involves forming of alloys in the semi-solid state and combines the advantages of drop-forging and casting. The minimum solidification shrinkage makes it possible to produce intricate, complexly designed components with great precision and obtain near-net-shaped products by means of the SSP [3−8].

Thixocasting is one of the most commonly used processes of semi-solid processing which involves the non-dendritic billets reheated at semi-solid temperatures and then billets injected in a closed die [3−8]. The alloy must have been non-dendritic structure for semi-solid forming. In this state, the alloy shows thixotropic behavior. This behavior can be defined that the shear rate increases and the viscosity decreases with increasing time. Thixocasting offers significant processing advantages, such as near net shape manufacturing, good surface finish, low energy consumption and high operating efficiency improvement [3−8]. And also thixocasting offers forming of the wrought aluminum alloys [11−20].

Authors had examined the thixoformability, artificial aging heat treatment, microstructure and mechanical properties of AA7075 alloy produced by semi-solid processing [12−17,21−26]. Researchers emphasized that the artificial aging heat treatments improved the mechanical properties of wrought aluminum alloys produced by semi-solid processing [11,12,16,17,21−23]. Recent studies showed that the AA7075 alloy was successfully formed by semi-solid

Corresponding author: Volkan KILICLI; Tel: +90-312-2028761; Fax: +90-312-2028947; E-mail: vkilicli@gazi.edu.tr
DOI: 10.1016/S1003-6326(16)64223-1

processing [12−17]. A few investigations have been done about the tensile fracture behavior of A356 aluminum alloy produced by semi-solid processing [27−30]. No efforts have so far been made to investigate the tensile fracture behavior of thixocast AA7075 alloy. But a few papers were concentrated on hot tensile deformation and fracture behavior of Al−Zn−Mg−Cu alloy [31]. At present, the detailed microstructural characteristics have not been correlated with the tensile fracture behavior and mechanical properties of thixocast AA7075 alloy.

The present study aims to investigate the effect of thixocasting process and T6 artificial aging heat treatment on the tensile fracture behavior of AA7075 aluminum alloy. In order to make a comparison, the as-extruded AA7075 alloy was also investigated.

2 Experimental

The chemical composition of a commercial AA7075 aluminum alloy, used in the present study, is given in Table 1. The AA7075 alloy was obtained in the condition of as-extruded (extrusion ratio of 1:5) and T651 (solution heat treated, stress relieved by stretching and artificially aged) alloys.

Table 1 Chemical composition of AA7075 wrought aluminum alloy used in this study (mass fraction, %)

Zn	Mg	Cu	Mn	Si	Cr	Fe	Al
5.599	2.033	1.329	0.183	0.383	0.157	0.741	Rest

Seiko 6200 model differential thermal analysis (DTA) was used to determine the solidification interval and the liquid fraction-temperature relationship. Approximately 20 mg samples were heated up to 660 °C at the heating rate of 10 °C/min. The change of liquid fraction with temperature was obtained from the heat flow versus temperature curves, as shown in Fig. 1.

Before thixocasting, feedstocks were prepared by SIMA (strain induced melt activation process) process. Specimens were cut from the as-extruded AA7075 alloy with 40 mm diameter into 60 mm height and then subjected to 30% cold working by using 200 t hydraulic press.

The photograph and schematic view of experimental set-up for thixocasting process were represented in Fig. 2(a) and Fig. 2(b), respectively. In the previous studies, vertical press was generally used for thixoforming [11,12,14−16]. On the contrary, in the present study, horizontal cold chamber high pressure die casting machine (HPDC) was used with the intention of using industrial applications. For this reason, an induction coil and billet holder mechanism was attached to HPDC machine as can be seen from Fig. 2(a).

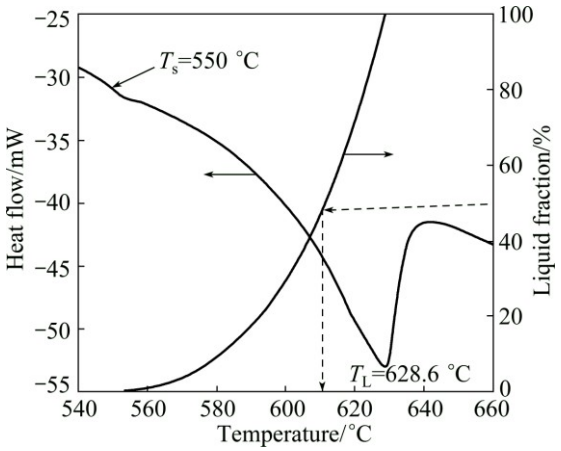

Fig. 1 Relationship among heat flow, liquid fraction and temperature of AA7075 alloy

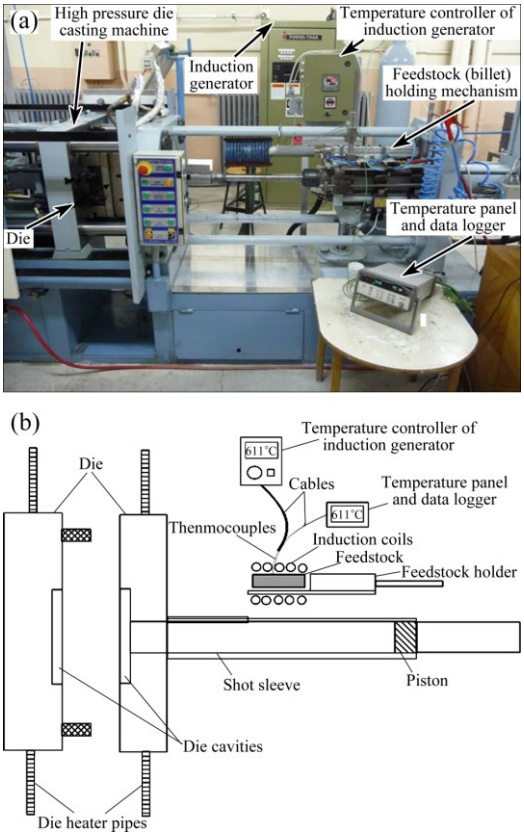

Fig. 2 Experimental set-up of HPDC machine for thixocasting process: (a) Photography; (b) Schematic representation

Thixocasting process was conducted at a cold chamber HPDC with medium frequency induction heating generator. Thixocasting of specimens was carried out at 611 °C which corresponds to the 50% liquid fraction and constant die temperature (150 °C) and injection speed (2.37 m/s).

Thixocast part and metallographic specimen sectioned regions are shown in Figs. 3(a) and (b), respectively. For the metallographic examination, specimens were prepared by standard metallographic

procedures and polished with up to 0.1 μm colloidal silica and etched with Keller's reagent. Microstructural features were studied using Leica DM4000M optical microscope and Jeol JSM 6060LV scanning electron microscope (SEM) with attached energy-dispersive X-ray spectroscopy (EDS) analysis of IXRF systems.

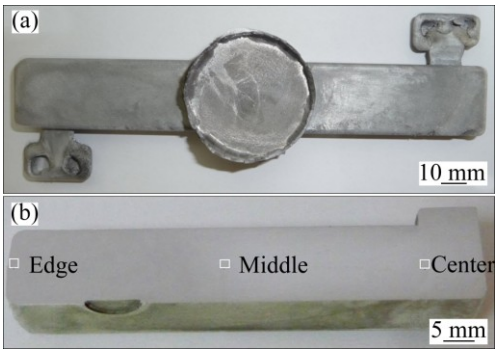

Fig. 3 AA7075 alloy part produced by thixocasting (a) and metallographic examination regions of thixocast specimen (b)

For the T6 artificial heat treatment, thixocast specimens were solution-treated at 465 °C for 16 h and quenched in water at room temperature, and then artificially aged at 120 °C for 24 h.

Tensile and hardness tests were performed to characterize the mechanical properties of specimens formed by thixocasting. Preparation steps of tensile specimens are shown in Fig. 4. First of all, the thixocast parts were cut by wire electro discharge machine (WEDM) longitudinally into two parts (Fig. 4(a)) and then each part was cut transversely into 13 mm × 13 mm × 72 mm rectangular shape (Fig. 4(b)) and machined by turning (Fig. 4(c)). The dimensions of the tensile test specimens corresponding to standard ASTM E 8M [32] are given Fig. 5.

Tension tests were carried out at room temperature using an Instron 3369 machine with 50 kN loading

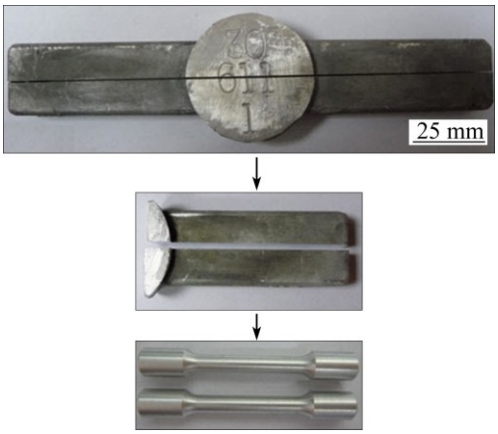

Fig. 4 Machining of tensile test specimen from thixocast AA7075 alloy

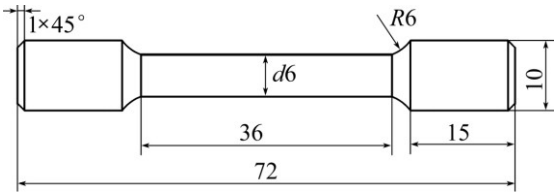

Fig. 5 Dimensions of tensile test specimens (unit: mm)

capacity at a cross-head speed of 1 mm/min. An extensometer set to a gauge length of 30 mm was used for strain measurement. An automatic record of stress versus elongation was made. At least five tensile specimens were tested for each condition and average values were calculated. Hardness tests were conducted in Emco Duravision 200 model universal hardness tester with a load of 5 kg. Hardness values were taken from the edge to the center of specimen. At least ten indents were made at each location and average values were taken.

Fracture surfaces of the tensile specimens were examined using the scanning electron microscope. In order to examine microstructure, crack initiation and final fracture tensile tests specimens were sectioned parallel to the tensile loading direction using a WEDM. The sectioned specimens were ground and polished, and then etched in Keller's reagent for metallographic examination.

3 Results and discussion

3.1 Microstructural evaluation

The optical micrographs of AA7075 alloy in as-extruded condition are shown in Fig. 6. Intermetallics were elongated in extrusion direction (Fig. 6(a)). In the case of transverse section of micrographs, the intermetallics showed rounded shape and well dispersed in α(Al) matrix (Fig. 6(b)). The fine dark and light gray intermetallics are considered to be $MgZn_2$ and $FeAl_3$, respectively [2].

The optical micrographs of the as-thixocast specimens sectioned from edge, middle and center positions showed homogeneous distribution of fine, equiaxed, near-globular grains (Fig. 7). On the contrary, in the middle and center regions, liquid-rich zone was observed near the surface (Figs. 8(b) and (c)). As a result of liquid segregation, micro-shrinkages appear in the sharp corner of specimen (Figs. 8(d) and (e)). The reason of this result may be attributed to the sharp corner of die. The sharp corner of die caused the liquid segregation during thixocasting [14,32]. To eliminate the liquid segregation, low liquid fractions were suggested during the thixocasting [14]. In the present study, these regions were removed by machining in order to prevent affecting the tensile properties adversely.

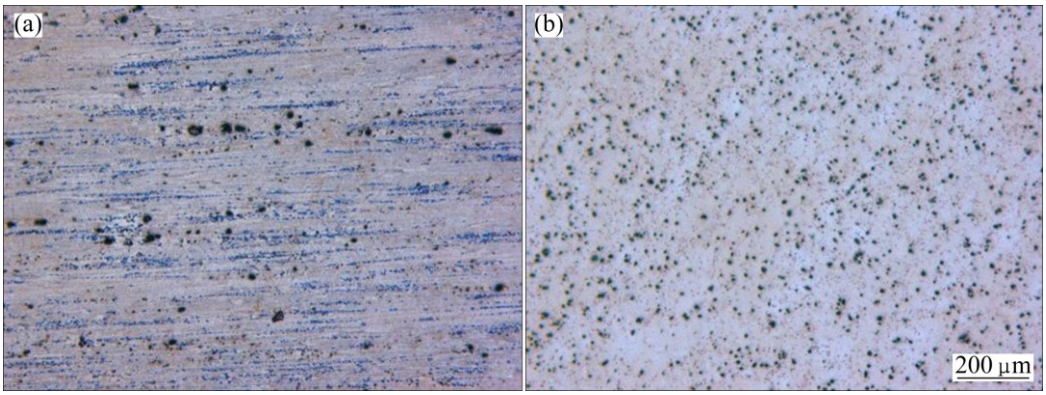

Fig. 6 Optical micrographs of AA7075 alloy in as-extruded condition: (a) Extrusion direction; (b) Transverse section

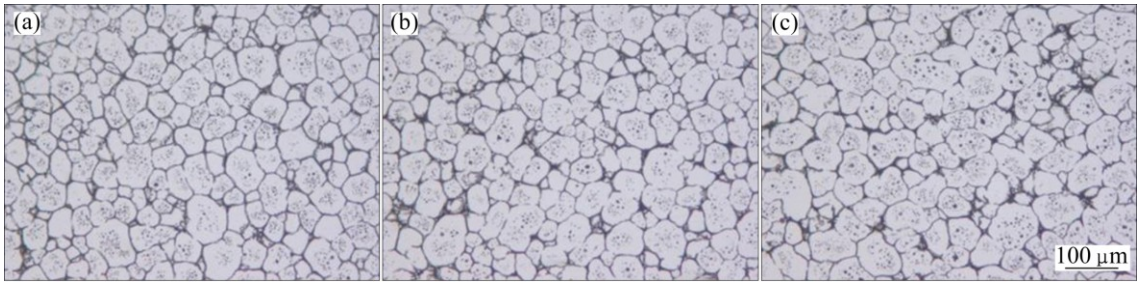

Fig. 7 Optical micrographs of as-thixocast AA7075 alloy: (a) Edge; (b) Middle; (c) Center

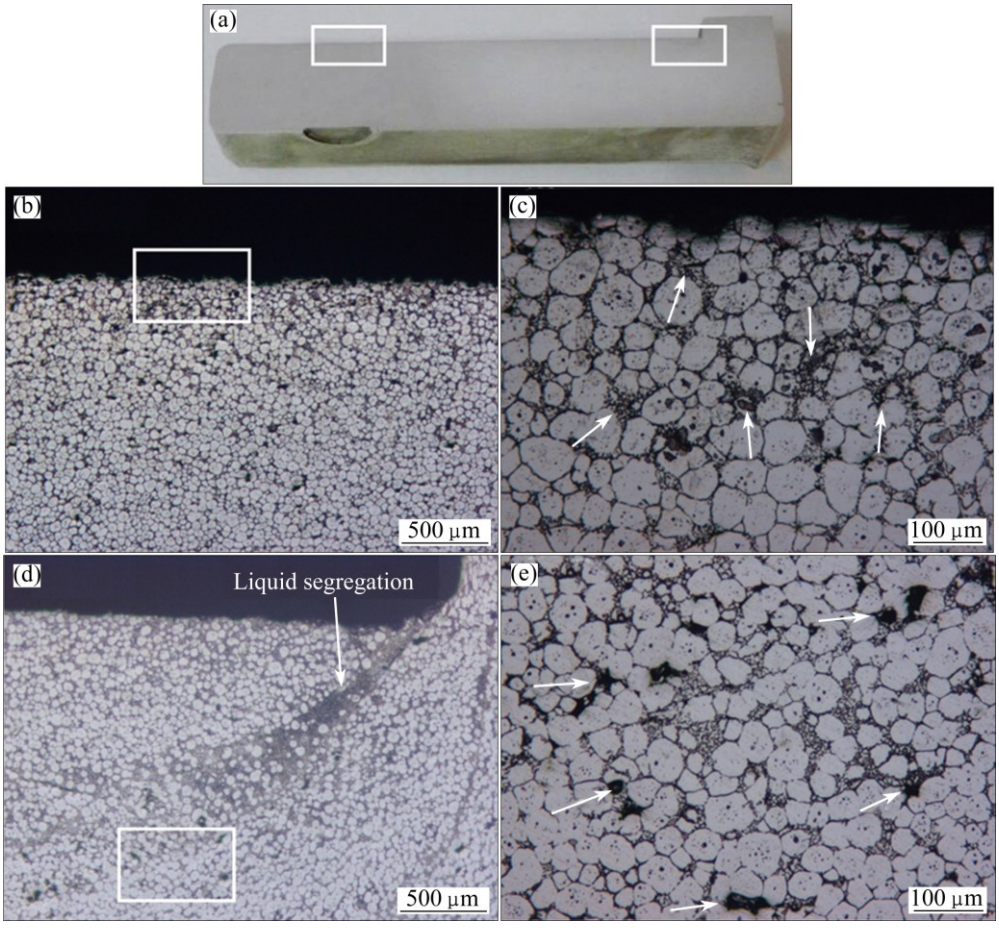

Fig. 8 Optical micrographs of as-thixocast specimens: (a) Longitudinally section of examined specimen; (b, c) Near surface region (arrows indicate liquid-rich zones); (d, e) Sharp corner of specimens (arrows indicate micro-shrinkages)

The microstructures of the as-thixocast specimen with micro-porosities and micro-shrinkages are shown in Fig. 9 and Fig. 10, respectively. Most of the micro-porosities were located in the triple junction of the primary α grains due to lack of liquid phase in the triple junction since the liquid phase wetted the primary α grain boundaries with capillary action, the triple junctions did not feed properly due to exhausted liquid phase [16,17]. There was no extra liquid phase or liquid feeder in order to feed liquid phase remained at grain boundaries in thixocasting. During solidification, liquid phase shrinkaged and it caused the formation of micro-shrinkages in microstructures. CHAYONG et al [12] reported that the presence of micro-shrinkages could be attributed to the liquid feeding which does not supply properly in semi-solid region during thixoforming of AA7075 specimen.

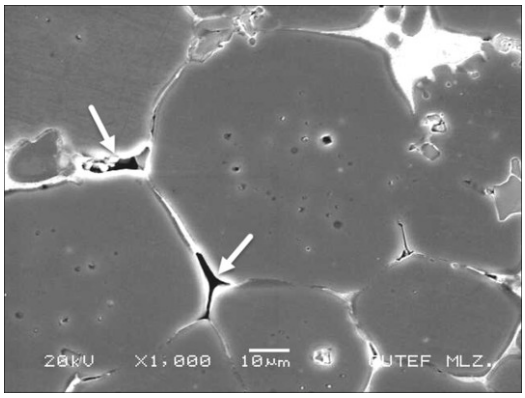

Fig. 9 SEM micrograph of micro-porosity in as-thixocast specimen (arrows indicates micro-porosities)

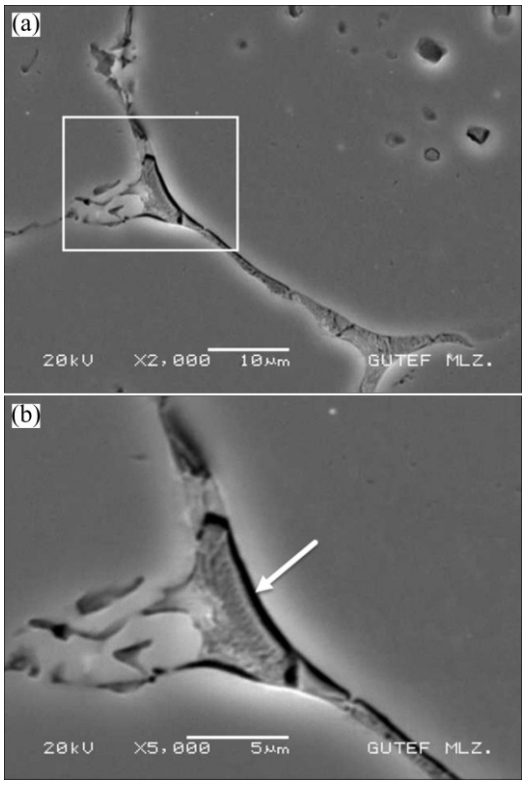

Fig. 10 SEM micrographs of micro-shrinkages in as-thixocast AA7075 specimen (arrows indicates micro-shrinkages): (a) Lower magnification; (b) Higher magnification

Figure 11 illustrates the SEM micrograph and EDS analyses of the as-thixocast AA7075 specimen. From this figure, it can be seen that a small amount of intermetallics appeared as black dots and were entrapped inside the globules (Fig. 11). By EDS analyses, the compositions of these intermetallics were identified as $Mg(Zn, Cu, Al)_2$ and Mg_2Si (Fig. 11, points 3 and 4). The intermetallics were entrapped inside by the primary α(Al) during thixocasting [21]. Since eutectic structure contains most of alloying elements, the globules matrix consisted of Al and a very small amount of Cu, Mg and Zn (Fig. 11, point 1). Moreover, Al−Cu−Zn−Mg multinary eutectic structure has been observed at primary α(Al) grain boundaries (Fig. 11, point 2). EDS analyses showed that eutectic structure in primary α(Al) grain boundary consisted of Al−Cu−Zn−Mg (Fig. 11, point 2). Similarly, researchers reported that the Mg_2Si inside the primary α(Al) globes and copper-rich eutectic structure were observed in thixoformed AA7075 alloy [21,22].

SEM micrograph and EDS analysis of thixocast + T6 specimen are illustrated in Fig. 12. The intermetallic inside the globules almost disappeared in thixocast + T6 specimen. The Si content of primary α(Al) is 0.275% in as-thixocast specimen (Fig. 11, point 1), after T6 heat treatment, the Si was not detected in primary α(Al) in EDS analysis (Fig. 12, point 1). EDS analyses revealed that the compositions of these intermetallics Mg_2Si (Fig. 12, point 3) and $Mg(Zn, Cu, Al)_2$ (Fig. 12, point 2) were identified (Fig. 12, point 3). The Mg_2Si formed at the triple junctions (Fig. 12, point 3). The prolonged solution treatment at 465 °C resulted in incipient melting which led to the formation of Mg_2Si intermetallics [22]. On the other hand, the prolonged solution time reduced the liquid segregation occurring during thixoforming [12]. The eutectic structure in primary α(Al) grain boundary initially presented in as-thixocast specimen. However, the eutectic structure was not observed at grain boundary in thixocast+T6 specimen. The non-equilibrium and low melting point eutectics were dissolved during the solution treatment [12].

3.2 Mechanical properties

The average yield strength, ultimate tensile strength (UTS), elongation and hardness values of the as-extruded, as-thixocast, thixocast+T6 specimens are given in Table 2. Among the tensile tested specimens, the as-extruded specimen exhibited the best combination of higher strength and ductility. This result is in good agreement with previous studies [11,12,33]. The as-thixocast

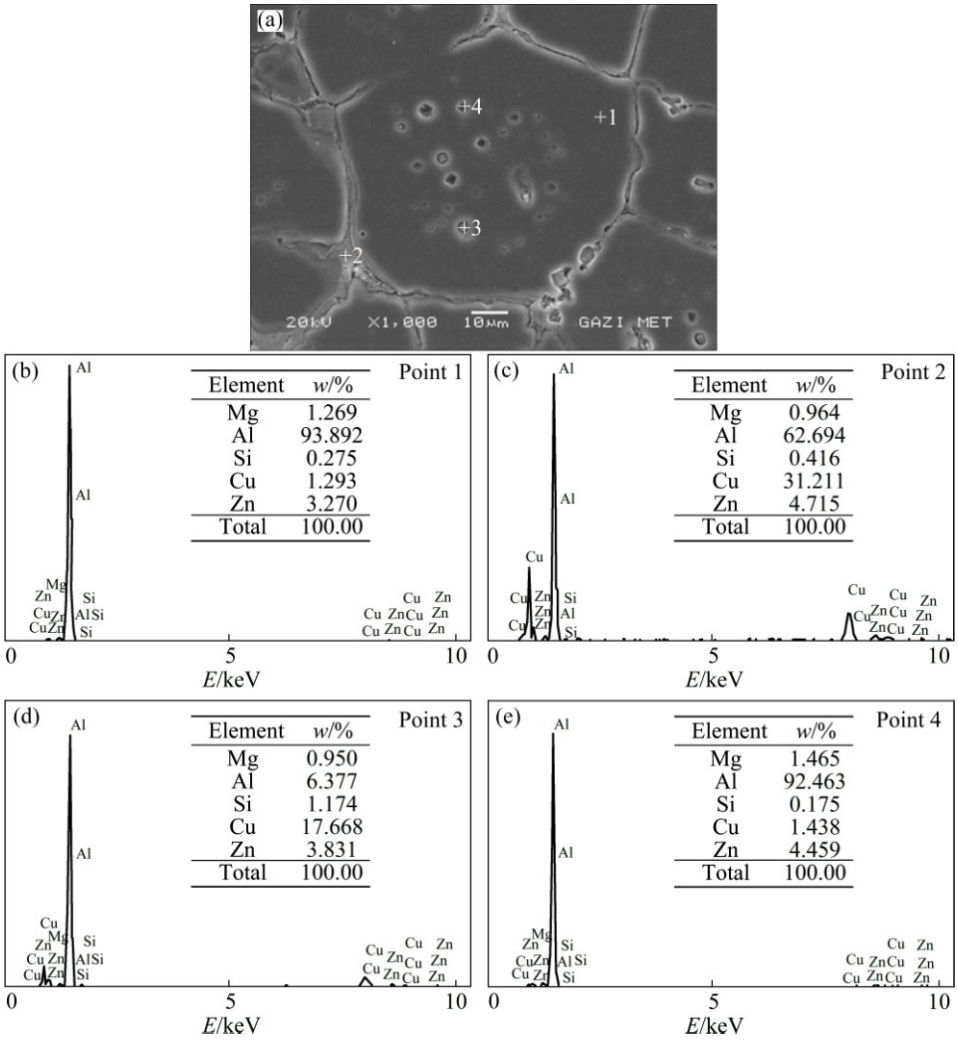

Fig. 11 SEM micrograph (a) and EDS analyses (b−e) of as-thixocast specimen

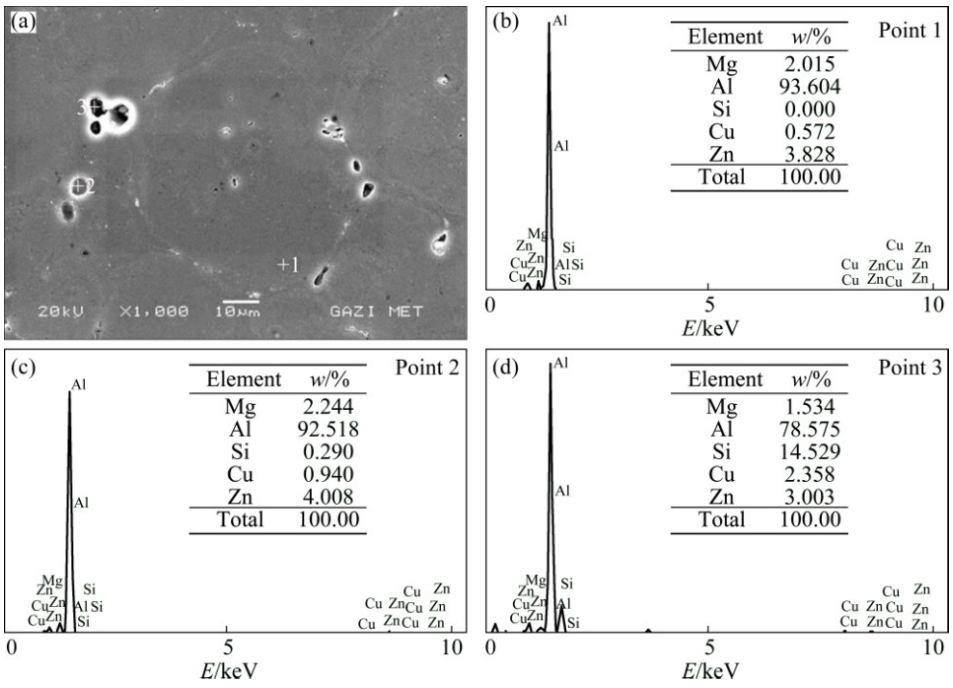

Fig. 12 SEM micrograph (a) and EDS analyses (b−d) of thixocast+T6 specimen

Table 2 Mechanical properties of tested specimens

Specimen	Yield strength/ MPa	Ultimate tensile strength/ MPa	Total elongation/ %	Hardness (HV, 5 kg)
As-extruded	375.6±8.3	519.7±14.7	13.1±0.8	106±2.5
As-thixocast	152.5±7.4	267.6±16.0	6.1±1.1	96.1±2.5
Thixocast +T6	342.1±11.0	511.3±5.9	12.5±1.9	115±3.4

specimen has lower tensile properties than the as-extruded specimen. The reason for this is attributed to the presence of micro-porosity and micro-shrinkages in microstructure of the as-thixocast specimen [12,14,16, 34]. In the present study, micro-porosities in the triple junction, micro-shrinkages and eutectic structure at primary α(Al) grain boundaries in the as-thixocast specimens were observed (Figs. 9 and 10)

The aging heat treatment of thixocast+T6 specimen improved the tensile properties which almost reached the tensile properties values of the as-extruded specimens (Table 2 and Fig. 13). Similar results were reported that the T6 heat treatments improved the mechanical properties and particularly enhanced the ductility of thixocast 7075 alloy [12,34]. The long-time solution treatment of thixocast aluminum alloy should be performed to dissolve non-equilibrium and low melting temperature phases completely and liquid segregation was reached its lowest value. Consequently, the UTS and total elongation values were enhanced [12,16,34].

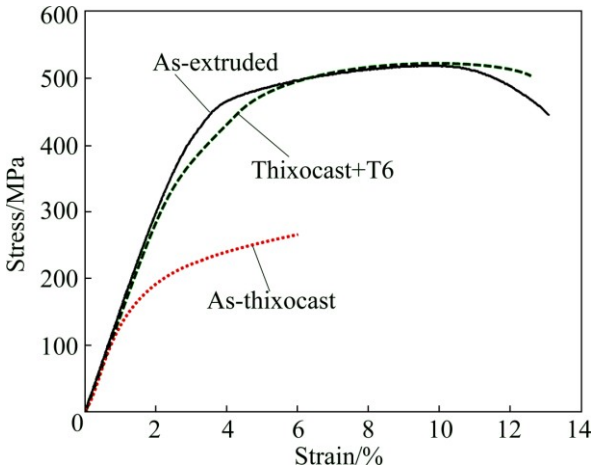

Fig. 13 Tensile curves of specimens

The hardness values of the as-thixocast and thixocast+T6 specimens were very low when compared with the as-extruded specimens (Table 2). Low hardness values in the as-thixocast specimen increased by T6 heat treatment as a result of precipitation hardening [16,34].

3.3 Tensile fracture behavior

SEM fractographs of the tensile fractured specimens of as-extruded, as-thixocast and thixocast+T6 specimens are given respectively in Figs. 14(a)−(c). The as-extruded specimen fracture type was ductile with the evidence of large and small dimples (Fig. 14(a)). The other fracture type in as-thixocast specimen was brittle (Fig. 14(b)). The brittle fracture occurred around the spheroidal grain due to micro-shrinkage and micro-porosity in microstructures (in Figs. 9 and 10). Quasi-cleavage fracture which is one of the brittle fracture modes has been observed in the as-thixocast specimen (Fig. 14(b)). This fracture mode is distinguished by separation of individual grains along [20].

In thixocast+T6 specimen, fracture type is ductile indicating the presence of the dimples (Fig. 14(c)). The large fractions of dimples were observed on the fracture surface of the as-extruded specimens (Fig. 14(a)) As mentioned before, the highest elongation among the tested specimens was obtained with thixocast + T6 specimens (Table 2).

The longitudinal sectional micrograph of necked region of the as-extruded specimen is shown in Fig. 15. In this region, initial void formation starts between the intermetallic compound and matrix (Fig. 15(a)) or interface of fractured intermetallic compound (Fig. 15(b)). The similar observations were made in previous studies [31,35,36].

In the as-thixocast specimen, the presence of micro-cracks around the globules is remarkable on the fracture surfaces of specimens (Fig. 16). Fracture has occurred around the spheroids due to micro-shrinkages (Fig. 10). In this specimen, the fracture mode is intergranular and decohesion starts between the interface of eutectic structure and primary α (Fig. 17). Previous study of ESKIN et al [10] showed that the fracture mode was intergranular due to Cu, Mg and Zn segregation at grain boundaries. It was determined that decohesion and micro-void formed at triple junction and between the eutectic and matrix interface, and the micro-void propagated along the grain boundaries (Fig. 17). CHAYONG et al [12] reported that, micro-void formed along the grain boundaries and decohesion began to around the globular grains.

In the thixocast + T6 specimen, initial micro-void formation started at Mg_2Si intermetallic compound and propagated along the grain boundaries (Fig. 18). Intermetallics such as Mg_2Si cause stress concentration, as indicated by arrows in Fig 18. The micro-voids nucleated at localized strain zone with associated intermetallics, secondary hard particles and inclusions [34]. These results are parallel to results of previous studies [28,29,31,37,38].

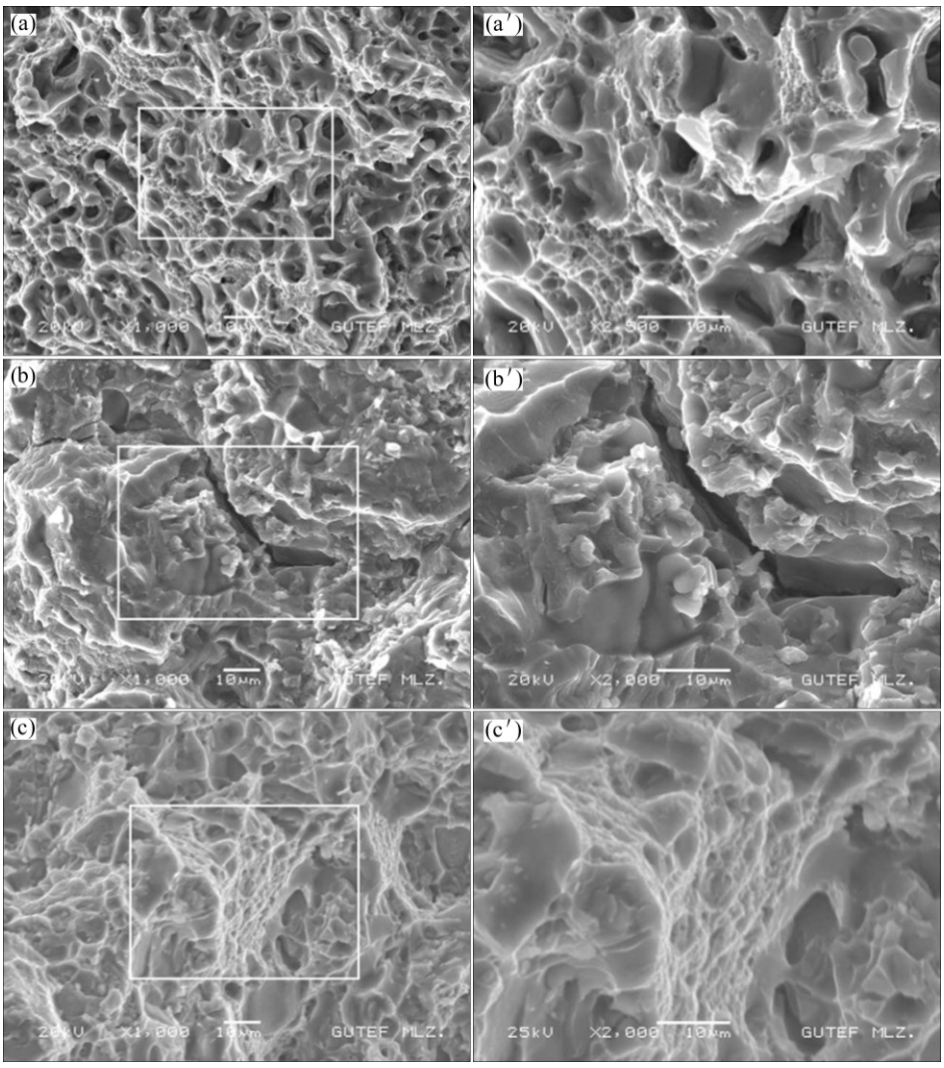

Fig. 14 SEM fractographs of specimens: (a,a′) As-extruded; (b,b′) As-thixocast; (c,c′) Thixocast+T6

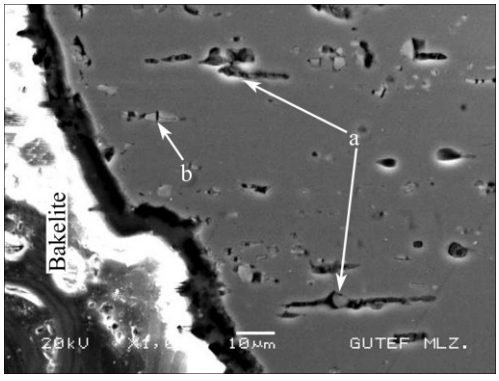

Fig. 15 Longitudinal sectional micrograph of as-extruded specimen (Arrow a: Initial void formation between the intermetallic compound and matrix; arrow b: initial void formation at the interface of fractured intermetallic compound)

4 Conclusions

1) In the thixocast+T6 specimen, the intermetallics entrapped inside the primary α and Mg_2Si intermetallics formed at grain boundaries during thixocasting.

2) The tensile properties of the as-thixocast AA7075 alloy were lower than those of the as-extruded and thixocast+T6 specimens.

3) T6 artificial heat treatment with prolonged solution treatment improved the tensile properties of the thixocast 7075 specimens.

4) The tensile properties of the as-extruded and thixocast+T6 specimens were close to each other.

5) The as-thixocast alloy exhibited dominant form quasi-cleavage fracture type and the presence of micro-cracks was remarkable. In this specimen, the mode was intergranular and decohesion started between the interface of eutectic structure and primary α grains.

6) The fracture types in the as-extruded and thixocast+T6 specimens are ductile with the evidence of dimples. In these specimens, initial void formation started between the intermetallic compound and matrix or interface of fractured intermetallic compound. In these alloys, fracture mode was also intergranular type.

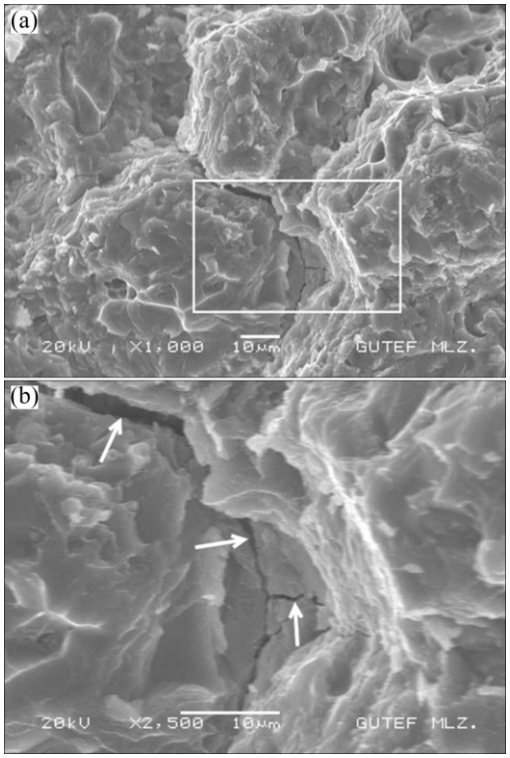

Fig. 16 Intergranular fracture mode in as-thixocast specimen: (a) Lower magnification; (b) Higher magnification (arrows indicate the micro-cracks along grain boundaries)

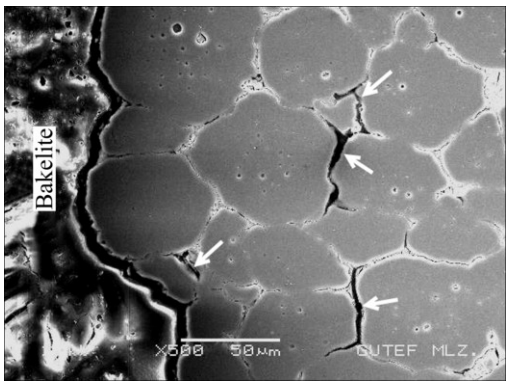

Fig. 17 Micro-void formation and propagation in as-thixocast specimen

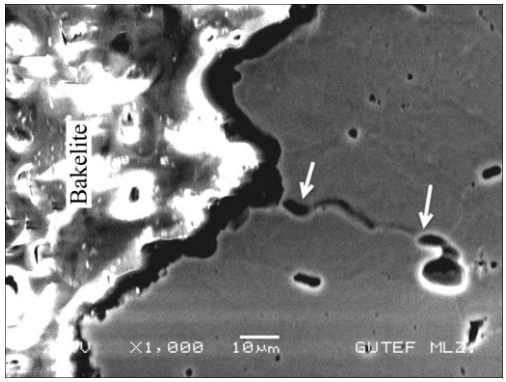

Fig. 18 Micro-void formation and propagation in thixocast+T6 specimen

Acknowledgement

The authors wish to acknowledge for the financial supports of the State Planning Organization of Turkey (DPT Project Number: 2003K120470-27) and Gazi University Scientific Research Fund (GUBAP Project Number: 07/2013-01).

References

[1] HATCH J E. Aluminum: Properties and physical metallurgy [M]. USA: Aluminum Association, ASM International, 1984.

[2] KAUFMAN J G. Introduction to aluminum alloys and tempers [M]. USA: ASM International, 2000.

[3] FLEMINGS M C. Behavior of metal alloys in the semisolid state [J]. Metallurgical and Materials Transactions B, 1991, 22: 269−293.

[4] KIRKWOOD D H. Semisolid metal processing [J]. International Materials Reviews, 1994, 39: 173−189.

[5] FAN Z. Semisolid metal processing [J]. International Materials Reviews, 2002, 47: 49−85.

[6] ATKINSON H V. Modelling the semisolid processing of metallic alloys [J]. Progress in Materials Science, 2005, 50: 341−412.

[7] ATKINSON H V. Semisolid processing of metallic materials [J]. Materials Science and Technology, 2010, 26: 1401−1413.

[8] KENNEY M P, COURTOIS J A, EVANS R D, FARRIOR G M, KYONKA C P, KOCH A A, YOUNG K P. Semisolid metal casting and forging [M]//Metals Handbook, USA: ASM International, 1988.

[9] HIRT G, KOPP R. Thixoforming [M]. Weinheim: Wiley-VCH Verlag Gmb H & Co., 2009.

[10] ESKIN D G, KATGERMAN L. Mechanical properties in the semi-solid state and hot tearing of aluminium alloys [J]. Progress in Materials Science, 2004, 49: 629−711.

[11] LIU D, ATKINSON H V, KAPRANOS P, JIRATTITICHAROEAN W, JONES H. Microstructural evolution and tensile mechanical properties of thixoformed high performance aluminium alloys [J]. Materials Science and Engineering A, 2003, 361: 213−224.

[12] CHAYONG S, ATKINSON H V, KAPRANOS P. Thixoforming 7075 aluminium alloys [J]. Materials Science and Engineering A, 2005, 390: 3−12.

[13] LEE Sang-yong, LEE Jung-hwan, LE Young-seon. Characterization of Al 7075 alloys after cold working and heating in the semi-solid temperature range [J]. Journal of Materials Processing Technology, 2001, 111: 42−47.

[14] VANEETVELD G, RASSILI A, LECOMTE-BECKERS J, ATKINSON H V. Thixoforging of 7075 aluminium alloys at high solid fraction [J]. Solid State Phenomena, 2006, 116: 762−765.

[15] ATKINSON H V, KAPRANOS P, LIU D, CHAYONG S A, KIRKWOOD D H. Thixoforming of normally wrought aluminium alloys [J]. Materials Science Forum, 2002, 396: 131−136.

[16] BURKE K J, ATKINSON H V, MCLELLAND A R A. Thixoforming of aluminium 7075 [C]//Proc 5th Int Conf Semi-Solid Processing of Alloys and Composites. Golden, Colorado, USA, 1998: 549−556.

[17] TURKELI, A, AKBAS N. Formation of non-dendritic structure in 7075 wrought aluminum alloy by SIMA process and effect of heat treatment [C]//Proc 4th Int Conf Semi-Solid Processing of Alloys and Composites. Sheffield, UK, 1996: 71−74.

[18] AKAR N, MUTLU I. Effect of predeformation rate in SIMA process on thixotropic structure of AA2024 aluminium alloy [J]. Journal of the Faculty of Engineering and Architecture of Gazi University, 2010, 25: 663−670.

[19] TANEROGLU H, AKAR N, KILICLI V. Examination of microstructure and mechanical properties of Al2024 alloy produced by thixocasting [J]. Journal of the Faculty of Engineering and

Architecture of Gazi University, 2013, 28: 803−809.
[20] AKAR N. The effect of reheating temperature on the production of thixotropic structure with SIMA process in AA2024 alloy [J]. Journal of the Faculty of Engineering and Architecture of Gazi University, 2011, 26: 381−388.
[21] MAHATHANINWONG N, WISUTMETHANGOON S, PLOOKPHOL T, WANNASIN J. Influence of solution heat treatment on microstructures of semisolid cast 7075 aluminium alloy [J]. Advanced Materials Research, 2011, 339: 371−374.
[22] MAHATHANINWONG N, PLOOKPHOL T, WANNASIN J, WISUTMETHANGOON S. T6 heat treatment of rheocasting 7075 Al alloy [J]. Materials Science and Engineering A, 2012, 532: 91−99.
[23] ROGAL L, DUTKIEWICZ J, GÓRAL A, OLSZOWSKA-SOBIERAJ B, DAŃKO J. Characterization of the after thixoforming microstructure of a 7075 aluminium alloy gear [J]. International Journal of Material Forming, 2010, 3: 771−774.
[24] ZHU W Z, MAO W M, QIN T U. Preparation of semi-solid 7075 aluminum alloy slurry by serpentine pouring channel [J]. Transactions of Nonferrous Metals Society of China, 2014, 24(3), 954−960.
[25] ZHOU B, KANG Y L, ZHU G M, GAO J Z, QI M F, ZHANG H H. Forced convection rheoforming process for preparation of 7075 aluminum alloy semisolid slurry and its numerical simulation [J]. Transactions of Nonferrous Metals Society of China, 2014, 24(4), 1109−1116.
[26] ROMETSCH P A, ZHANG Y, KNIGHT S. Heat treatment of 7xxx series aluminium alloys — Some recent developments [J]. Transactions of Nonferrous Metals Society of China, 2014, 24(7), 2003−2017.
[27] CAVALIERE P, CERRI E, LEO P. Effect of heat treatments on mechanical properties and fracture behavior of a thixocast A356 aluminum alloy [J]. Journal of Materials Science, 2004, 39: 1653−1658.
[28] BOOSTANI A F, TAHAMTAN S. Fracture behavior of thixoformed A356 alloy produced by SIMA process [J]. Journal of Alloys and Compounds, 2009, 481: 220−227.
[29] TAHAMTAN S, BOOSTANI A F, NAZEMI H. Mechanical properties and fracture behavior of thixoformed, rheocast and gravity-cast A356 alloy [J]. Journal of Alloys and Compounds, 2009, 468: 107−114.
[30] BOOSTANI A F, TAHAMTAN S. Effect of a novel thixoforming process on the microstructure and fracture behavior of A356 aluminum alloy [J]. Materials and Design, 2010, 31: 3769−3776.
[31] ZHOU M, LIN Y C, DENG J, JIANG Y Q. Hot tensile deformation behaviors and constitutive model of an Al−Zn−Mg−Cu alloy [J]. Materials and Design, 2014, 59: 141−150.
[32] ASTM E8, Standard test methods for tensile testing of metallic materials, annual book of ASTM standards [S].
[33] KIRKWOOD D H, SUÉRY M, KAPRANOS P, ATKINSON H V, YOUNG K P. Semi-solid processing of alloys [M]. Berlin: Springer-Verlag, 2009.
[34] MOHAMMADI H, KETABCHI M, KALAKI A. Microstructural evolution and mechanical properties of back-extruded Al 7075 alloy in the semi-solid state [J]. International Journal of Material Forming, 2012, 5: 109−119.
[35] KOBAYASHI T. Strength and fracture of aluminum alloys [J]. Materials Science and Engineering A, 2000, 280: 8−16.
[36] HUO W, HOU L, CUI H, ZHUANG L, ZHANG J. Fine-grained AA 7075 processed by different thermo-mechanical processings [J]. Materials Science and Engineering A, 2014, 618: 244−253.
[37] DENG J, LIN Y C, LI S S, CHEN J, DING Y. Hot tensile deformation and fracture behaviors of AZ31 magnesium alloy [J]. Materials and Design, 2013, 49: 209−219.
[38] LIN Y C, DENG J, JIANG Y Q, WEN D X, LIU G. Hot tensile deformation behaviors and fracture characteristics of a typical Ni-based superalloy [J]. Materials and Design, 2014, 55: 949−957.

触变铸造 AA7075 合金的拉伸断裂行为

Volkan KILICLI, Neset AKAR, Mehmet ERDOGAN, Kadir KOCATEPE

Department of Metallurgical and Materials Engineering, Faculty of Technology,
Gazi University, 06500 Teknikokullar, Ankara, Turkey

摘　要：研究了触变铸造、触变铸造+T6 人工时效以及挤压态 AA7075 合金的拉伸断裂行为。采用光学显微镜和扫描电子显微镜研究了合金的显微组织和断口形貌。结果表明，挤压态和触变铸造+T6 人工时效的合金具有比触变铸造合金更优越的力学性能。延长固溶时间后 T6 人工时效可使触变铸造 AA7075 合金的拉伸性能大大提高。挤压态和触变铸造+T6 人工时效合金的拉伸性能相近。触变铸造合金中存在明显的微裂纹，其断裂形式为晶间脆断。而挤压态和触变铸造+T6 合金的断裂形式为韧性断裂。对于触变铸造合金，破坏始于共晶基体界面之间，并在晶间扩展。微孔缩聚是触变铸造+T6 人工时效合金的主要断裂模式。而微孔形核于基体与多元共晶组织的界面。

关键词：AA7075 合金；半固态工艺；触变铸造；拉伸断裂行为；拉伸性能

(Edited by Yun-bin HE)